Subharmonic ferroresonance in an LCR circuit with hysteresis

H. LAMBA* M.GRINFELD* S.McKEE* R. SIMPSON†

Abstract

We use the Preisach model of magnetic hysteresis to model the inductance in a series LCR circuit. By introducing a hysteresis parameter into the Preisach functions used, we are able to continuously vary the width of the hysteresis loop and thereby investigate the effects of magnetic hysteresis on the circuit's behaviour. In particular, it is shown that the stability region of a period-3 subharmonic ferroresonant solution can increase significantly as the hysteresis losses are reduced. The bifurcations leading to the appearance and disappearance of this subharmonic solution are examined. Also strong numerical evidence is provided for the unsuitability of single-valued $M-H$ curves in the analysis of ferroresonant phenomena.

1 Introduction

The study of magnetic circuits is of great importance in electrical engineering. Many of these circuits are highly nonlinear allowing coexisting stable solutions. This may lead to sudden and dramatic changes in the response when the system is disturbed. This phenomenon, which is known as *ferroresonance*, requires the use of nonlinear dynamics methods.

A sinusoidally-driven series LCR circuit is one of the simplest circuits capable of ferroresonant behaviour and has been studied previously [1, 2, 3, 4, 5] as a model for a single-phase transformer. In particular, Teape et. al. [6] noted the existence of a stable subharmonic ferroresonant solution with a period three times that of the forcing, over a relatively small range of input voltages. In this paper we identify the bifurcations leading to the appearance and disappearance of this solution.

Many models have been used to represent the M–H characteristic and these can be broadly classified into two groups. Firstly the magnetization can be described

*Department of Mathematics, University of Strathclyde, Glasgow G1 1XH, UK.
†Department of Electronic and Electrical Engineering, University of Strathclyde, Glasgow G1 1XQ, UK.
This research was supported by the EPSRC, Research Grant number GR/J69417.

by a single-valued function of the applied magnetic field, e.g. by linear, piecewise-linear, polynomial or trigonometric functions. Using such functions it is possible to apply analytic methods such as harmonic balance to obtain results on the amplitudes and regions of stability of certain types of ferroresonant solution [1, 3, 5, 7, 8, 9]. However, to predict ferroresonant behaviour in a circuit it is important that the magnetization characteristic of the inductor is accurately modelled since this is the only nonlinearity in the system.

The second group of models, which are much closer to the observed behaviour of real materials, include magnetic hysteresis effects and are therefore no longer representable by single-valued functions. Examples are the Preisach [10] and Jiles-Atherton models [11]. These models suffer from two drawbacks. Firstly it is much harder to accurately fit an experimentally-determined magnetic characteristic and secondly the resulting circuit equations are likely to be analytically intractable.

We use the Preisach model to simulate numerically a series LCR circuit (the same method can of course be applied to more complicated circuits). Our representation of the magnetization characteristic allows us to smoothly vary the width of the hysteresis loop (i.e. reduce the ferromagnetic hysteresis losses) while keeping the other magnetic characteristics approximately constant. In this way the effects of magnetic hysteresis in ferroresonant circuits, and the consequences of neglecting it, can be also explored. This is achieved by choosing a class of Preisach models with a single hysteresis parameter, ϵ, such that when $\epsilon = 0$ the model reduces to a single-valued relationship, namely the sum of hyperbolic tangent functions, between the magnetization of the inductor and the applied magnetic field. Increasing ϵ increases the width of the hysteresis loop for $0 \leq \epsilon \leq 1$ (see § 2.1). Of particular interest is the stability region of the ferroresonant solutions as ϵ is varied.

The paper is organized as follows. In § 2 we describe the Preisach model and our choice of Preisach functions. In § 3 the equations for a series LCR circuit are derived, showing how to incorporate the Preisach model and integrate the equations numerically. In § 4 the bifurcations causing the appearance and disappearance of the period-3 subharmonic ferroresonance are identified. Bifurcation diagrams, with ϵ as bifurcation parameter, are given in § 5 for a parameter regime where a period-3 subharmonic ferroresonance occurs. We also show that this subharmonic ferroresonance does not occur for these parameter values in the $\epsilon = 0$ single-valued representation together with an extra resistor, in parallel with the inductor, representing transformer losses. This strongly suggests that even for a qualitative understanding of ferroresonant circuits, a hysteretic inductance must be used in the simulations.

2 The Preisach model

The Preisach model [10] is still one of the best mathematical descriptions of magnetic hysteresis available. A detailed description of the model and its numerical implementation can be found in [12]. Here we outline only that part of the theory necessary for the rest of this paper.

Let us denote the applied magnetic field by $H(t)$ and the magnetization of the material by $M(t)$. The magnetic material is assumed to be a superposition (or infinite sum) of elementary loops $\gamma_{\alpha,\beta}$, called hysterons, shown in Figure 1. The functions $\gamma_{\alpha,\beta}(H(t))$ can take the values $+1$ or -1, switching at the values $H = \alpha$ and $H = \beta$. The magnetization M is then defined to be

$$M(H(t)) = \iint_{\alpha \geq \beta} w(\alpha, \beta)\, \gamma_{\alpha,\beta}(H(t))\, d\alpha\, d\beta$$

where $w(\alpha, \beta)$ is a non-negative weight function describing the distribution of the hysterons. In addition $w(\alpha, \beta) = w(-\beta, -\alpha)$, in order to preserve the symmetry of the hysteresis loops with respect to positive and negative applied fields, and $w(\alpha, \beta)$ decays sufficiently fast as $|\alpha|, |\beta| \to \infty$ so that the magnetization saturates at a finite value.

Insert Figure 1 here

The state of the magnetic material at some time T is defined by all the values $\gamma_{\alpha,\beta}(T)$, and not just the magnetization M which is simply a weighted average taken over all the elementary loops. In fact the state of the material can be described by a diagram in the (α, β) plane and depends only upon the extrema of $H(t)$ for $t < T$. Assume that at some previous time $t_0 < T$ the material was in a state of complete negative magnetization, i.e. $H = -\infty$ and $\gamma_{\alpha,\beta} = -1 \;\forall\; \alpha, \beta$. Then as H is increased to some value H_1, say, all the hysterons with $\alpha < H_1$ will flip to $+1$. If H is then decreased to a value H_2 those hysterons that have already flipped once will flip back to -1 if $\beta > H_2$. If H is now increased to above H_1 then all memory of the last two turning points is erased and the material behaves exactly as though the turning point at H_1 had not occurred. This is known as the 'wiping-out property' and is very close to the observed behaviour of magnetic materials.

More generally, let us denote the set of hysterons in the $+1$ state at time t by $S^+(t)$ and those equal to -1 by $S^-(t)$. Therefore,

$$M(H(T)) = \iint_{S^+} w(\alpha, \beta)\, d\alpha\, d\beta - \iint_{S^-} w(\alpha, \beta)\, d\alpha\, d\beta.$$

As $H(t)$ evolves the boundary between S^+ and S^- is a 'staircase function' in the α-β plane consisting of horizontal and vertical line segments that evolves in time, as in Figure 2. This boundary can be thought of as representing the 'magnetic memory' of the material .

Insert Figure 2 here

For clarity, let us suppose that at some time t_0 the material is close to negative saturation i.e. $H(t_0)$ is large and negative, and let $H(t_0) = e_0$. Then at some time

$T > t_0$ the set of maxima $\{E_i\}_{i=1}^{i=n_1(T)}$ and minima $\{e_i\}_{i=1}^{i=n_2(T)}$ of $H(t)$ that contribute to $M(T)$ (i.e. that have not been wiped out) are defined inductively by

$$E_1 = \max_{[t_0,T]} H(t), \qquad H(t_1^+) = E_1,$$

$$e_1 = \min_{[t_1^+,T]} H(t), \qquad H(t_1^-) = e_1,$$

and

$$E_k = \max_{[t_{k-1}^-,T]} H(t), \qquad H(t_k^+) = E_k,$$

$$e_k = \min_{[t_k^+,T]} H(t), \qquad H(t_k^-) = e_k.$$

Insert Figure 3 here

The times $\{t_i^+\}_{i=1}^{i=n_1}$m and $\{t_i^-\}_{i=1}^{i=n_2}$ denote the times at which these maxima and minima occur as shown in Figure 3. Note that if $H(T)$ is increasing, then $n_1(T) = n_2(T) - 1$, otherwise $n_1(T) = n_2(T)$.

Now we define the function $F(\alpha', \beta')$

$$F(\alpha', \beta') = \int_{\beta'}^{\alpha'} \left(\int_{\beta}^{\alpha'} w(\alpha, \beta)\, d\alpha \right) d\beta \tag{1}$$

which is the integral of the function w over a triangle in the α, β plane. In [12] it is shown that the magnetization at time t is defined in terms of $F(\alpha, \beta)$ and for decreasing H,

$$\begin{aligned} M(t) &= -\lim_{\alpha \to \infty} F(\alpha, -\alpha) + 2 \sum_{k=1}^{n_1(t)-1} \left[F(E_k, e_{k-1}) - F(E_k, e_k) \right] \\ &\quad +2 \left[F(E_{n_1}, e_{n_1-1}) - F(E_{n_1}, H(t)) \right] \end{aligned} \tag{2}$$

and for increasing H it is given by

$$\begin{aligned} M(t) &= -\lim_{\alpha \to \infty} F(\alpha, -\alpha) + 2 \sum_{k=1}^{n_1(t)-1} \left[F(E_k, e_{k-1}) - F(E_k, e_k) \right] \\ &\quad +2F(H(t), e_{n_1-1})). \end{aligned} \tag{3}$$

From (2) and (3) it is clear that knowledge of the function $F(\alpha, \beta)$ is sufficient to completely define the magnetic response. Defining the response in terms of F rather than w is computationally much more efficient since the integrals (1) no longer need to be evaluated.

The function F must satisfy certain conditions, namely

$$F(\alpha, \beta) = F(-\beta, -\alpha) \tag{4}$$

to preserve symmetry with respect to positive and negative saturation and

$$\lim_{\alpha\to\infty} F(\alpha,-\alpha) < \infty \tag{5}$$

to ensure that the hysteresis loop saturates at a finite value. In addition

$$\frac{\partial F}{\partial \beta} \leq 0, \quad \frac{\partial F}{\partial \alpha} \geq 0. \tag{6}$$

ensure that the magnetic permeability $\frac{dM}{dH} \geq 0$ everywhere.

2.1 Choice of the function $F(\alpha, \beta)$

A simple single-valued function with the necessary symmetry and saturation properties to represent a magnetic characteristic is the hyperbolic tangent function. In this case

$$F(\alpha,\beta) = \frac{M_s}{2}[\tanh(P\alpha) - \tanh(P\beta)] \tag{7}$$

where M_s is the saturation value and P is determines the saturation rate.

In order to obtain a hysteresis loop we modify (7) and instead define

$$\begin{aligned} F(\alpha,\beta) \quad &= \quad \frac{M_s}{2}[\tanh(P\alpha) - \tanh(P\beta) \\ &\quad -\frac{\epsilon}{2}(\operatorname{sech}^2(P\beta)\tanh(P\alpha) - \operatorname{sech}^2(P\alpha)\tanh(P\beta))] \end{aligned} \tag{8}$$

It is easily checked that for $0 \leq \epsilon \leq 1$, F satisfies conditions (4)–(6) (if $\epsilon > 1$ then conditions (6) are violated). The upper and lower curves of the hysteresis loop are given by

$$M = M_s[\tanh(PH) + \frac{\epsilon}{2}\operatorname{sech}^2(PH)]$$

$$M = M_s[\tanh(PH) - \frac{\epsilon}{2}\operatorname{sech}^2(PH)]$$

respectively. The remanence, M_r, and coercivity, H_c, of the material as functions of ϵ are the intersections of the outer loops with the lines $H = 0$ and $M = 0$ respectively and are given by

$$M_r = M_s\epsilon/2$$

and

$$H_c = \frac{1}{2P}\sinh^{-1}(\epsilon).$$

Note that as ϵ is increased the major hysteresis loop completely encloses the major loops for smaller ϵ. This property allows us to claim that the width of the hysteresis loop is being altered without significantly changing the other properties of the loop.

In fact a single hyperbolic tangent function is not a good representation for the hysteresis loops of many materials; however the functions defined in (8) can be added together to give

$$\begin{aligned} F(\alpha, \beta) &= \sum_{i=1}^{i=n} \frac{M_i}{2} \Big[\tanh(P_i \alpha) - \tanh(P_i \beta) \\ &\quad - \frac{\epsilon}{2} \left(\operatorname{sech}^2(P_i \beta) \tanh(P_i \alpha) - \operatorname{sech}^2(P_i \alpha) \tanh(P_i \beta) \right) \Big] \qquad (9) \end{aligned}$$

where $M_i > 0$, $\sum M_i = M_s$ and $P_i > 0$.

This describes a much larger class of hysteresis loops than is possible using (8) (conditions (4)-(6) still hold for $0 \leq \epsilon \leq 1$). In fact most 'soft' magnetic materials can be reasonably approximated in this way (the functions (9) appear to be unsuitable for hard materials). Using such functions it is possible to investigate ferroresonant circuits using the Preisach model in a computationally efficient way.

It should be emphasized that we are not proposing a method to precisely model the experimentally-determined hysteresis loops of magnetic materials. Nor are we suggesting that our method for smoothly deforming hysteresis loops is unique, but it will provide a qualitative understanding of the effects of magnetic hysteresis in magnetic circuits, and therefore the consequences of neglecting hysteresis.

3 A ferroresonant LCR circuit

Insert Figure 4 here

The equation for the series LCR circuit can be written as a set of first-order ordinary differential equations:

$$\frac{dH}{dt} = \frac{1}{nA} \left(V \sin(\omega t) - v_C - lRH/n \right) / (\mu_0 + \frac{dB}{dH}) \qquad (10)$$

$$\frac{dv_C}{dt} = Hl/Cn \qquad (11)$$

$$\frac{dB}{dt} = \frac{dB}{dH} \frac{dH}{dt} \qquad (12)$$

where the independent variables are the applied magnetic field H (A/m), the magnetic flux density B (Teslas) and v_C, the voltage across the transformer. The parameters are the mean flux path length l (m), the number of turns n on the transformer, the cross-sectional area A (m^2), the peak driving voltage V, the angular frequency $\omega = 2\pi f$, the resistance R (Ω) and the leakage inductance L (A/m). Note also that the current $i = lH/n$.

In order to close the system of equations we need to know $\frac{dB}{dH} = \frac{\mu_0}{A} \frac{dM}{dH}$. This is where the Preisach model and most of the computation comes in. This is calculated by differentiating the last term of (2) or (3) depending on whether H is decreasing or increasing, with $F(\alpha, \beta)$ defined by (9) for a particular choice of ϵ. Thus dB/dH is discontinuous whenever dH/dt changes sign. It is also discontinuous whenever a maximum or minimum is wiped out since the number of terms in (2) and (3) will change.

The equations were integrated using a variable-step method suitable for stiff systems. Whenever a discontinuous change in dB/dH occurs, the program must halt the integration, update the sets of extrema and then restart the integration. The initial conditions for the integration are the values of H and v_C at time $t = 0$, the point-of-wave of the forcing cycle and the sets of extrema $\{E_i\}$ and $\{e_i\}$ (i.e. the magnetic history of the material). In all the numerical computations reported here, the magnetic core was in fact assumed to be in an initially demagnetized state, so that the initial sets $\{E_i\}$ and $\{e_i\}$ were sequences respectively decreasing and increasing towards zero (this is similar to demagnetizing an inductor by applying a slowly-decreasing alternating magnetic field).

In [6] a subharmonic ferroresonance with a period of three times the forcing period was found in a series LCR circuit both experimentally and numerically (using a different hysteretic representation of the inductance). This period-3 solution is stable for a narrow voltage range and coexists with the nonresonant solution and a high amplitude ferroresonant solution, both with the same period as the forcing. Our intention here is re-examine this subharmonic behaviour, using the methods of nonlinear dynamics. In particular we are interested in the bifurcations leading to the appearance and disappearance of this solution as the driving voltage is varied. We can also, by our choice of Preisach function, examine the stability range of this solution as the hysteresis losses in the transformer are varied. This cannot of course be done experimentally but provides useful qualitative insights into the effect of magnetic hysteresis on the circuit's behaviour and the consequences of neglecting it in the modelling of the circuit.

Our parameter values and transformer characteristics (with $\epsilon = 1$) were chosen to match the circuit studied in [6]. The values used were $C = 6.8\mu F$, $R = 1.91\Omega$, $f = 50\text{Hz}$ with $n = 240$, $A = 0.0026\text{m}^2$ and $l = 0.434\text{m}$.

The transformer characteristic was fitted using (9) with two terms, one to match the permeability at low magnetization (M_1 and P_1), and the other to match the rate of saturation at high applied fields. A good match was found with the parameters $M_1 = 0.8 \times A/\mu_0$, $M_2 = 0.7 \times A/\mu_0$, $P_1 = 20$ and $P_2 = 2$. giving a flux density B that saturates at 0.7+0.8=1.5 Teslas. Using more terms in (9) it should be possible to obtain a better approximation to the transformer characteristic, but the qualitative agreement with just two terms is excellent, recreating the subharmonic behaviour observed experimentally at approximately the same range of driving voltages.

4 The bifurcations of the subharmonic ferroresonant solution

In this section, the hysteresis parameter ϵ is fixed at $\epsilon = 1$. This corresponds to a remanent flux density of $0.75T$ and a coercivity of $\approx 30A/m$.

Insert Figure 5 here

The bifurcation diagram for slowly-varying applied voltages is shown in Figure 5 and is similar to that found in [6]. For a large voltage range (between approximately 110V and 325V there are two coexisting stable period-1 solutions, a non-resonant (low amplitude) solution which is stable for voltages less than 325V and a very large amplitude (fundamental ferroresonant) solution where the inductor becomes saturated and which is stable above 110V. If the voltage is increased continuously from some low value (less than 110V) then the non-resonant solution is followed until at 325V the system jumps to the fundamental ferroresonance. If the voltage is then decreased, the fundamental ferroresonant solution will be followed until 110V when the system drops down to the non-resonant solution.

Within this voltage range there is a much smaller range – from approximately 217-245V in which the period-3 ferroresonant solution also exists. The current waveform is shown in Figure 6 and a plot of flux density B against current is shown in Figure 7.

Insert Figure 6 here

Insert Figure 7 here

The appearance or disappearance of a solution, or a change in its stability, is known as a bifurcation. It is therefore of interest to try and identify the bifurcations leading to the disappearance of the period-3 solutions above. An excellent introduction to bifurcation theory can be found in [13].

At approximately 245V the period-3 solution either loses stability or ceases to exist and the system abruptly jumps to the non-resonant solution (the system never jumps to the fundamental ferroresonant solution). The same sudden transition to the non-resonant solution is also observed experimentally. This is clear evidence of either a saddle-node bifurcation (where the period-3 solution ceases to exist) or a subcritical pitchfork bifurcation (where the solution loses stability). Proving which of these is in fact occurring is very difficult (see the discussion at the end of this section) but pitchfork bifurcations usually occur in the neighbourhood of trivial solutions in systems obeying some kind of symmetry condition. This is not the case here so it seems probable that the solution is disappearing at a saddle-node bifurcation.

At the lower end of the voltage range there is a period-doubling bifurcation and a more gradual loss of stability. Firstly the period-3 motion becomes a period-6. The sequence of bifurcations after this is very hard to analyze, but over a range of 3 to 4V at around 217V, the solution appears to lose its periodicity and perform small amplitude, seemingly random, oscillations about the period-3 solution — that is to say, the circuit behaves chaotically (see Figure 8) in a neighbourhood of the original period-3 solution before finally losing stability and moving to the non-resonant solution. This period-doubling and loss of periodicity was also observed experimentally.

Insert Figure 8 here

There is an important point to make about the bifurcations observed above. The use of the Preisach model results in a set of ODEs that depend discontinuously on the sequences of extrema $\{E_i\}$ and $\{e_i\}$ which in turn are modified as the system evolves. The resulting system is therefore not a dynamical system of standard type and the nature of the bifurcations is less clear. This is apparent when studying the small voltage range in the neighbourhood of the period-doubling bifurcation. The precise bifurcation sequence that is observed, and the bifurcation parameters, depend critically upon the previous history of the material and the rate at which the voltage V is swept. The discontinuous nature of the system also makes it impossible to use any of the available bifurcation packages, such as AUTO. Indeed the rigorous analysis of systems of this kind presents a considerable mathematical challenge.

5 The effect of decreasing hysteresis

As described in § 2, our choice of Preisach function allows us to decrease the width of the hysteresis loop — something that is impossible to do experimentally. Figure 9 shows the approximate voltage range for which the period-3 motion is stable as a function of ϵ. Interestingly, this voltage range *increases* as ϵ is initially decreased, the upper limit staying approximately constant while the period-doubling bifurcation occurs at decreasing values. This result is important if one is designing or modifying a system which is operated close to a ferroresonant region — changing the magnetic characteristics to reduce transformer losses may actually increase the stability region of the ferroresonant solutions.

Insert Figure 9 here

As the width of the loop is reduced still further, (below $\epsilon \approx 0.5$), a qualitative change occurs. The period-3 solution still exists (although it appears that only a very small set of initial conditions will lead to this motion) and at the same time new chaotic and quasiperiodic motions appear, replacing the non-resonant solution. Of course, the most obvious effect of reducing the width of the hysteresis loop is to reduce the transformer losses and so it is not surprising that for ϵ close to zero the behaviour of the numerical simulation changes dramatically.

Since the vast majority of numerical simulations in the literature use single-valued representations for the magnetic characteristic it is of great interest to see if, in our numerical model, by using $\epsilon = 0$ together with an extra load in the circuit to represent the transformer losses, we can recreate the dynamics close to $\epsilon = 1$ for the same circuit parameter values.

Therefore an extra resistance R_2 was added in parallel to the inductance in the circuit shown in Figure 4. The numerical simulation was then run repeatedly with R_2 varying. A detailed search failed to find the period-3 ferroresonance. This strongly suggests that the dynamics of the fully-hysteretic model with $\epsilon \approx 1$, which are in close qualitative agreement with the experimentally-observed behaviour, cannot be recreated with the single-valued representation $\epsilon = 0$ even if hysteresis losses are taken into account. This provides further evidence for the need to incorporate hysteresis into future numerical simulations of ferroresonant circuits.

6 Conclusions

In this paper we have numerically simulated a ferroresonant circuit using the Preisach model of magnetic hysteresis and obtained good agreement with experiment [6], even though our representation of the inductance was chosen primarily to enable us to reduce the hysteresis in a systematic way and not to fit the transformer values precisely. We then identified the bifurcations through which the subharmonic ferroresonance loses stability.

In addition, by our choice of Preisach function, we have been able to investigate the effects of magnetic hysteresis by observing the behaviour of the periodic solutions as the hysteresis parameter was reduced. Interestingly, our computations showed that a reduction in the width of the hysteresis loop initially resulted in a wider stability range for the subharmonic ferroresonant solution. As the hysteresis loop became closer to a single-valued representation, the low-amplitude motions were replaced by stable chaotic and quasiperiodic motions. Our numerical representation also enabled us to make a direct comparison between a fully hysteretic model and one in which the magnetic response was represented by a single-valued function plus transformer losses. Our results showed that the single-valued representation was not sufficient to recreate the subharmonic ferroresonance at the same parameter values and therefore casts severe doubt upon the use of such non-hysteretic representations, even in very simple ferroresonant circuits.

It is only recently that ferroresonance has been recognized and studied as a nonlinear phenomenon. The response of ferromagnetic materials to an applied magnetic field is both nonlinear and hysteretic and it is important to try to understand the contribution of each to the qualitative behaviour of the system. We believe that the methodology and results in this paper are a useful step in this direction.

There are still many questions to be asked about ferroresonance even in such a simple circuit. One obvious question is to examine the width of the stable subharmonic voltage region as a function of the capacitance C. Another very important question is to determine the effect of remanence in deciding which stable solution is reached. The use of a Preisach-like model is essential for this and is the subject of a forthcoming paper.

References

[1] J. R. Marti and A. C. Soudack. Ferroresonance in power systems: Fundamental solutions. *IEEE Proc. C*, 138:321–329, 1991.

[2] C. Kieny. Application of the bifurcation theory in studying and understanding the global behaviour of a ferroresonant electric power circuit. *IEEE Trans. Power Delivery*, 6:866–872, 1991.

[3] A. E. A. Araujo, A. C. Soudack, and J. R. Marti. Ferroresonance in power systems: chaotic behaviour. *IEEE Proc. C*, 140:237–240, 1993.

[4] J. H. B. Deane. Modelling the dynamics of nonlinear inductor circuits. *IEEE Transactions on Magnetics*, 30:2795–2801, 1994.

[5] S. K. Chakravarthy and C. V. Nayar. Ferroresonant oscillations in capacitor voltage transformers. *IEE Proceedings – Circuits, devices and systems*, 142:30–36, 1995.

[6] J. W. Teape, R. D. Slater, R. S. Simpson, and W. S. Wood. Hysteresis effects in transformers, including ferroresonance. *Proc. I.E.E.*, 123:153–158, 1976.

[7] M. S. Maklad and A. A. Zaky. Multimodal operation of a ferroresonant circuit with quintic nonlinearity. *IEEE Transactions on Magnetics*, 12:380–384, 1976.

[8] M. S. Maklad and M. M. Fahmy. An analytical investigation of a ferroresonant circuit. *IEEE Transactions on Magnetics*, 16:465–468, 1980.

[9] B. A. Mork and D. L. Stuehm. Application of nonlinear dynamics and chaos to ferroresonance in distribution systems. *IEEE Trans. Power Delivery*, 9:1009–1017, 1994.

[10] F. Preisach. On magnetic after-effect. *Zeitschrift Physik*, 94:277, 1935.

[11] D. C. Jiles and D. L. Atherton. Ferromagnetic hysteresis. *IEEE Transactions on Magnetics*, 19:2183–2185, 1983.

[12] I. D. Mayergoyz. *Mathematical models of hysteresis*. Springer-Verlag, New York, 1991.

[13] G. L. Baker and J. P. Gollub. *Chaotic Dynamics – an introduction*. CUP, Cambridge, 1990.

Captions for Figures

Figure 1: An elementary loop.

Figure 2: The sets S^+ and S^- in the (α, β) plane.

Figure 3: The sets $\{E_i\}$ and $\{e_i\}$.

Figure 4: A series LCR circuit.

Figure 5: Coexisting non-resonant, fundamental ferroresonant and period-3 ferroresonant solutions for $\epsilon = 1$. The peak current is plotted against the peak applied voltage.

Figure 6: The current waveform for the period-3 subharmonic ferroresonance.

Figure 7: A plot of flux density B (in Teslas) against current for the period-3 subharmonic ferroresonance.

Figure 8: A chaotic motion close to the period-3 solution as it loses stability at $217.5V$.

Figure 9: A sketch of the stability range of the period-3 solution as a function of the hysteresis parameter ϵ.

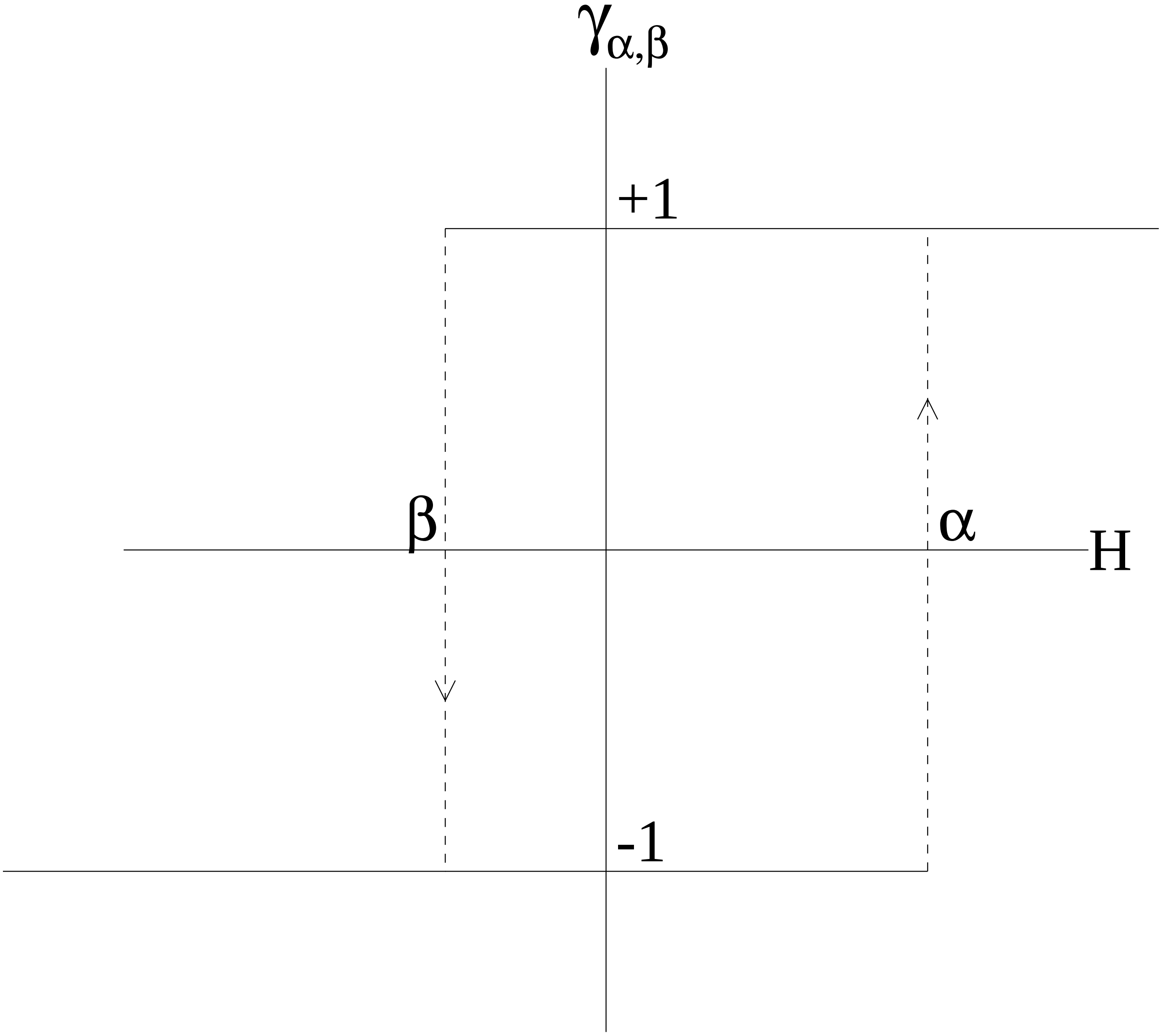

Figure 1: An elementary loop.

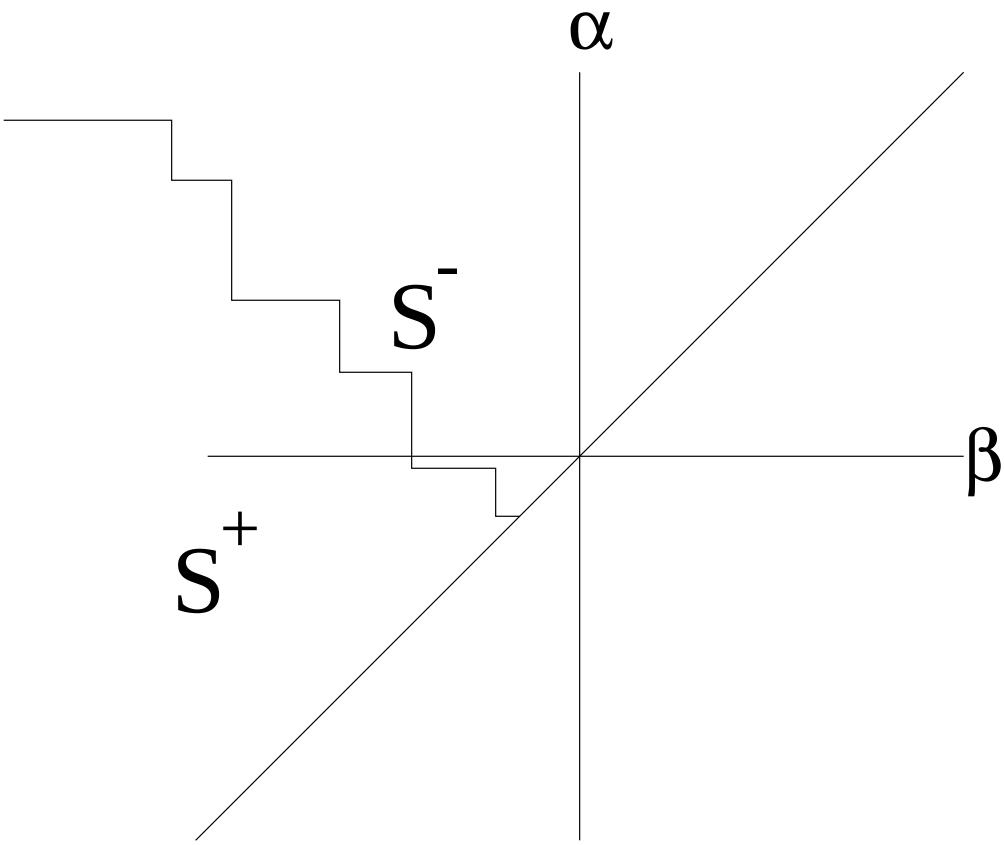

Figure 2: The sets S^+ and S^- in the (α, β) plane.

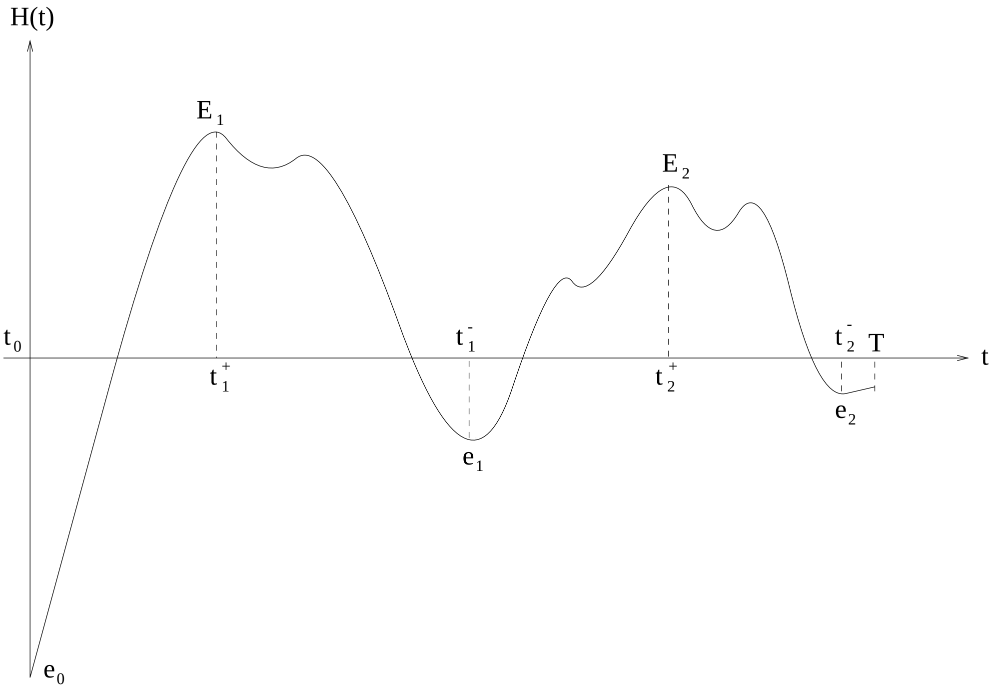

Figure 3: The sets $\{E_i\}$ and $\{e_i\}$.

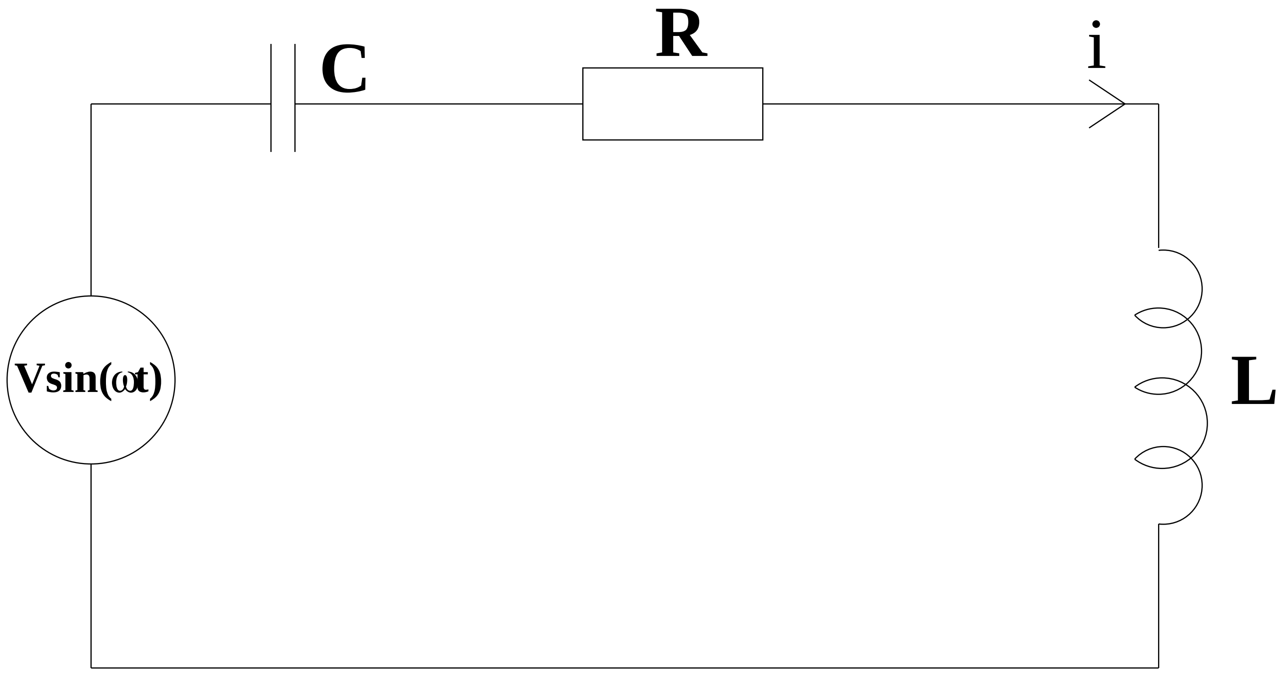

Figure 4: A series LCR circuit.

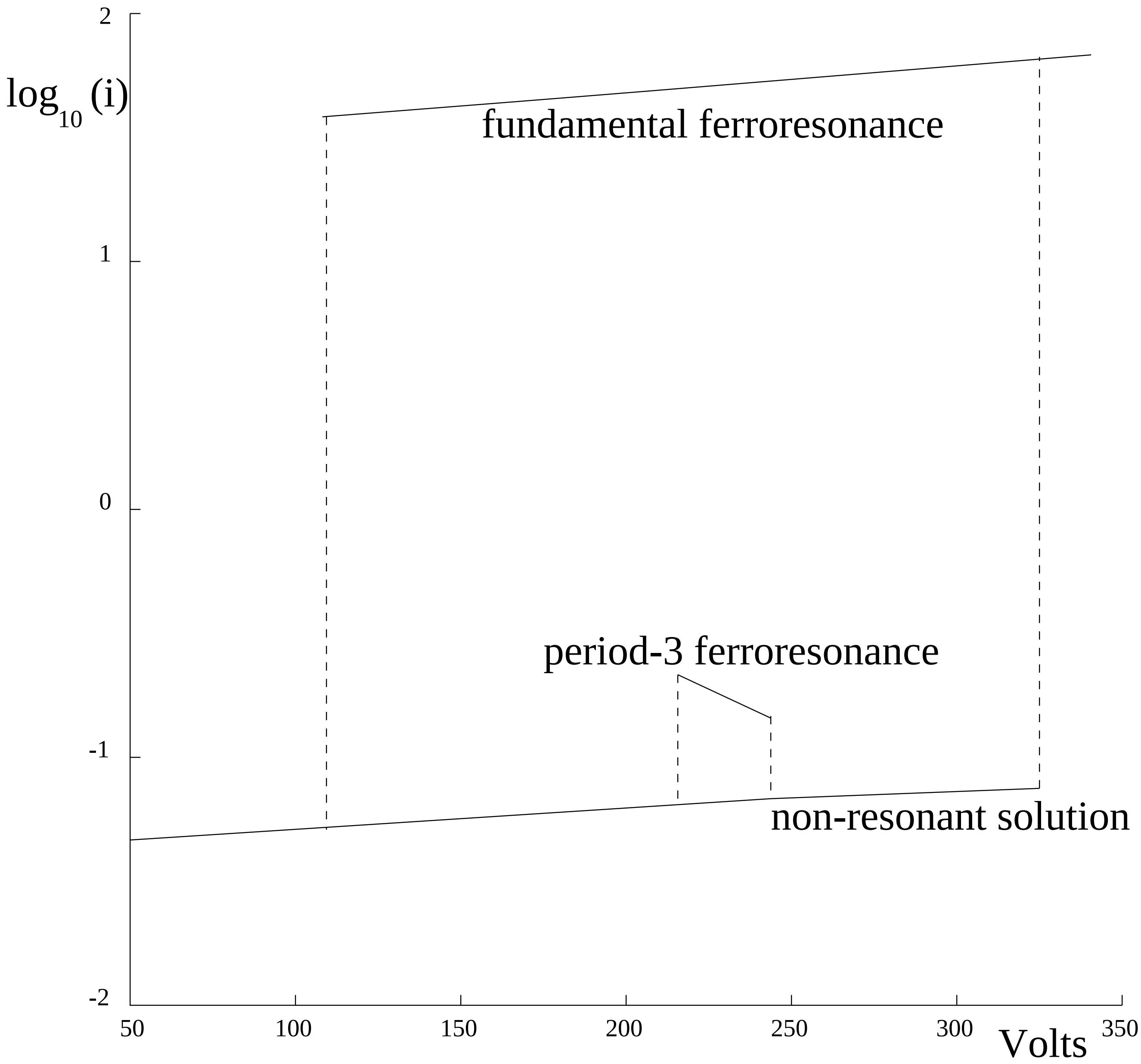

Figure 5: Coexisting non-resonant, fundamental ferroresonant and period-3 ferroresonant solutions for $\epsilon = 1$. The peak current is plotted against the peak applied voltage.

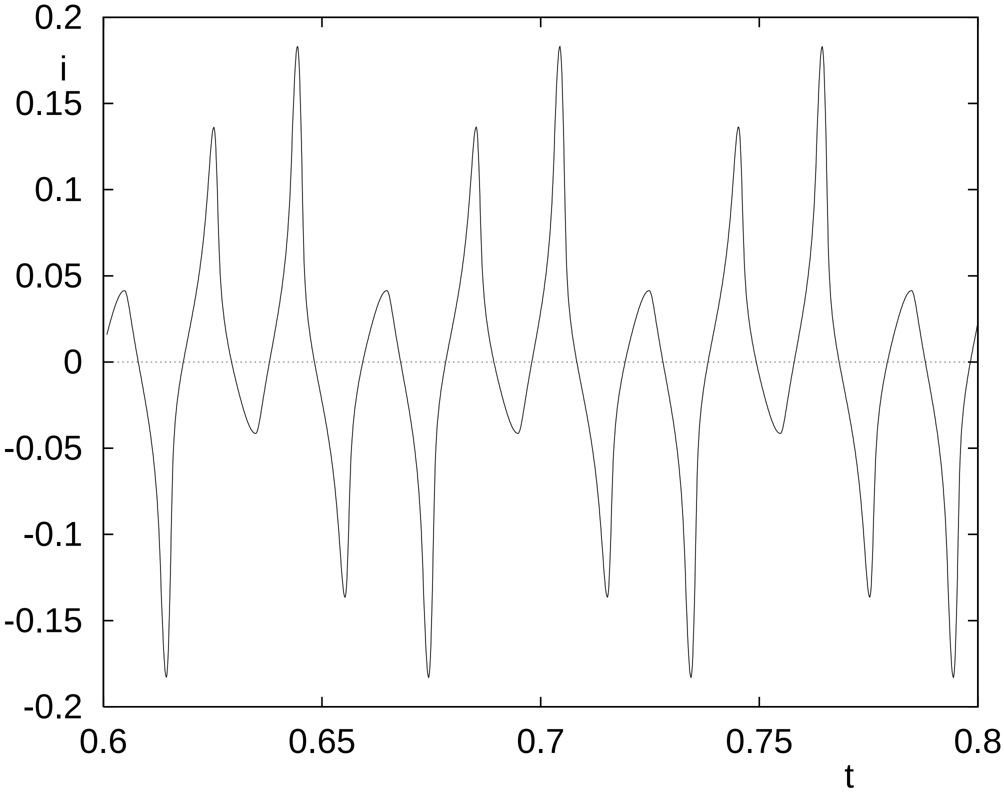

Figure 6: The current waveform for the period-3 subharmonic ferroresonance.

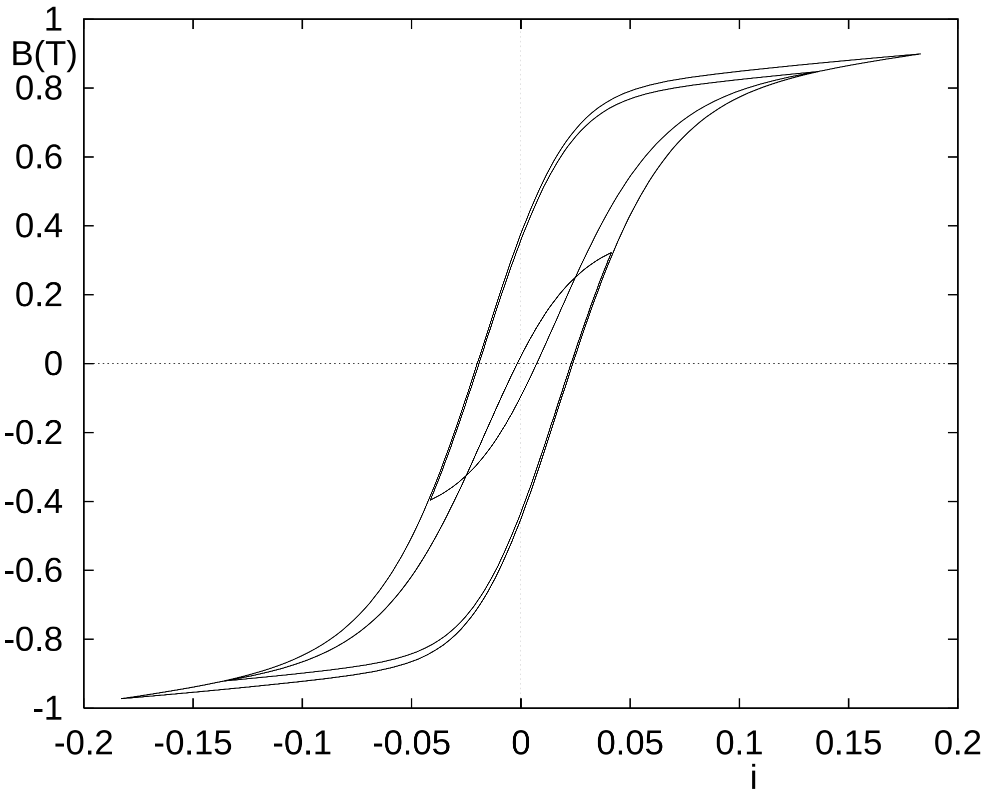

Figure 7: A plot of flux density B (in Teslas) against current for the period-3 subharmonic ferroresonance.

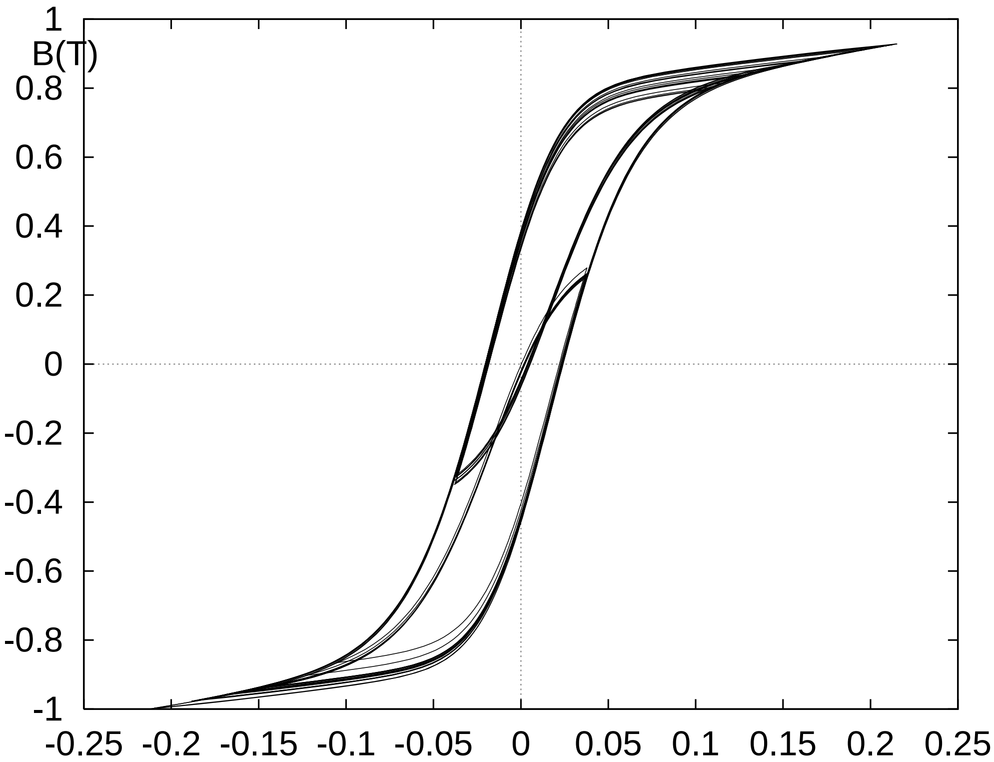

Figure 8: A chaotic motion close to the period-3 solution as it loses stability at $217.5V$.

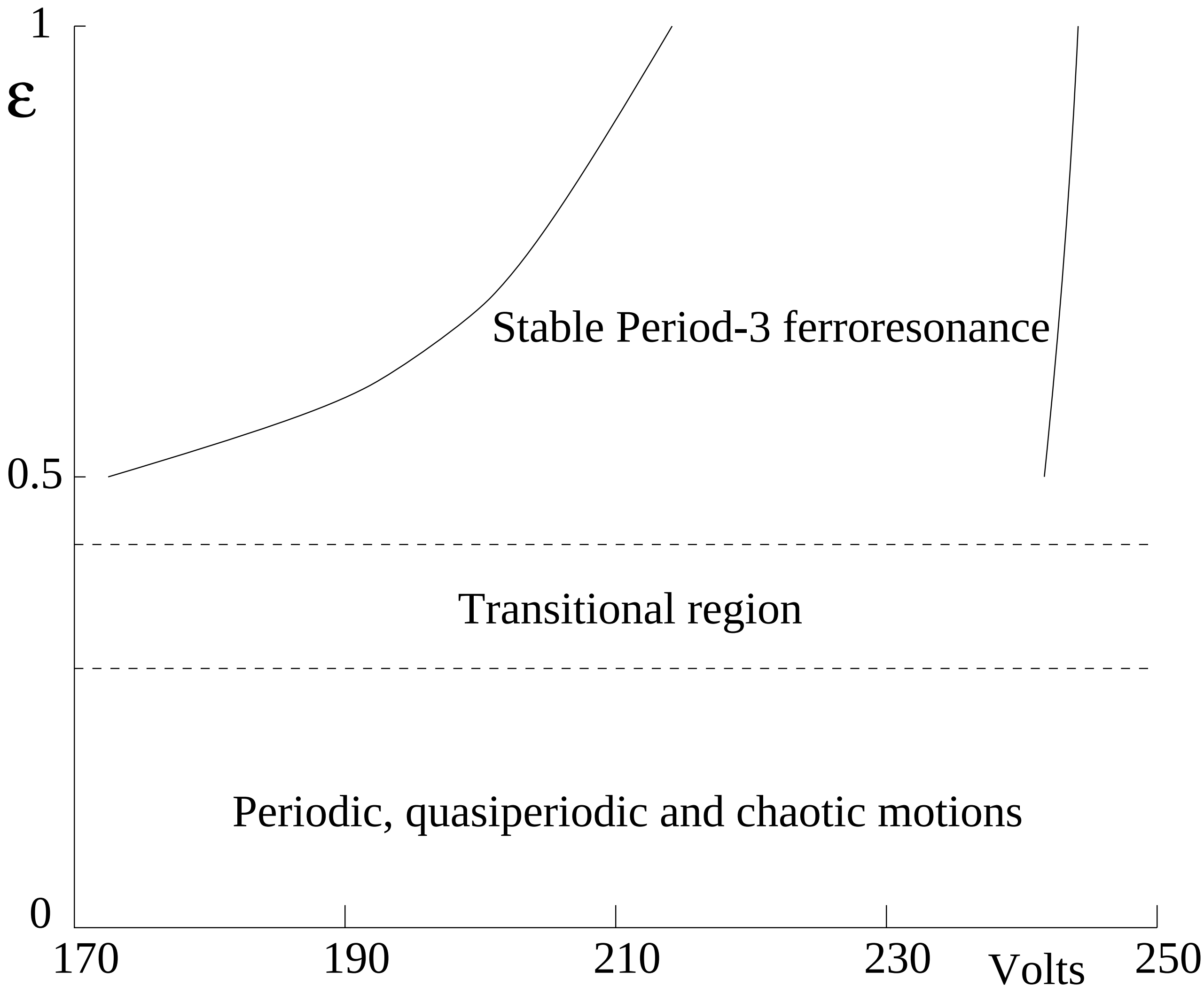

Figure 9: A sketch of the stability range of the period-3 solution as a function of the hysteresis parameter ϵ.